Single-photon modulation spectrum*

Liu Yan(刘 岩), Yu Bo(于 波), He Bo(何 博), Zhang Guo-Feng(张国峰),
Xiao Lian-Tuan(肖连团)†, and Jia Suo-Tang(贾锁堂)

State Key Laboratory of Quantum Optics and Quantum Optics Devices, Laser Spectroscopy Laboratory, Shanxi University, Taiyuan 030006, *China*

(Received 27 June 2013; revised manuscript received 23 September 2013; published 2 December 2013)

We present a robust method of single-photon modulation by directly modulating the single photons and observe its frequency spectrum. Compared with conventional photon counting technique, the single-photon modulation spectrum shows that the method could not only realize high-frequency modulation but also obtain higher signal-to-noise ratio. Moreover, the theoretical calculations show good agreement with the experimental results.

Keywords: signal-to-noise ratio, single-photon modulation, spectrum

PACS: 01.55.+b, 02.30.Cj, 02.30.Nw, 02.60.Ed **DOI:** 10.1088/1674-1056/23/1/010101

1. Introduction

The single-photon detection has been widely used, particularly in fields of quantum information, three-dimensional imaging, optical time-domain reflectometry,[1–6] etc. Photon counting has superior stability compared with analog signal measurement owing to its insensitivity to the variation of gain, and it leads to an obvious improvement in signal-to-noise ratio (SNR), which could often be exploited for the single-photon detection.[7–9] To the Poisson statistics source, the ideal photon counting situation shows the photon quantum noise, i.e., standard deviation $\sqrt{\bar{n}T}$, and SNR $= \bar{n}T/\sqrt{\bar{n}T} = \sqrt{\bar{n}T}$, where $\bar{n}$ is the mean photon number, and the T is the sample time. This is the ultimate SNR that one can ever expect which seriously affects the sensitivity of measurements. Although the SNR can be improved using longer sampling time T, it is unpractical in the dynamic measurements. In order to enhance the SNR, the photon counting modulation method[10–15] has been proposed in the weak-light measurements. Photon counting modulation converts the photon counts into analog signals that feed into an analog lock-in amplifier, detects the signal at a known modulation frequency in amplitude and phase, and then suppresses noise at other frequencies. It improves the SNR significantly and restrains the influence of the background noise effectively.[14] In a previous publication,[15] we demonstrated that the signal to noise improvement ratio reaches 31.7 dB by using photon counting modulation. However, the analog conversion makes it difficult for the photon counting modulation to measure a relatively small signal amplitude by normalizing it against the direct current background, and the low modulation frequency (< 10 Hz) used may make some infections from flicker noise ($1/f$ noise).

In this paper, we study the spectrum characteristics of the single-photon modulation (SPM) system by directly modulating the single photons, i.e., modulating the detection probability of the single photons. It is shown that the SPM method could work at high frequencies with high SNR.

2. Theoretical analysis

2.1. SPM theory

Unlike the conventional intensity modulation methods, the SPM aims at modulating the probability that a photon is detected by using an intensity modulator, which means to modulate the single-photon occurrence probability, and then detect by using a single-photon avalanche detector (SPAD) to generate a square wave pulse. When the incident photons are modulated by a sine wave, the probability for the photon to be detected is the biggest at the peak of the sine wave.

Mandel[16] first deduced the theoretical formula about the photon count statistics of the radiation field with the field intensity fluctuation, and the probability that n photons are emitted in a sampling time T can be expressed as

$$p(n,T) = \int_0^\infty \frac{(r_T T)^n}{n!} \mathrm{e}^{-r_T T} P(r_T)\,\mathrm{d}r_T, \tag{1}$$

and

$$r_T(t) = \frac{1}{T}\int_t^{t+T} [r_0 + \varepsilon f(\tau)]\,\mathrm{d}\tau, \tag{2}$$

where $r_T(t)$ is the effective photon emission rate over a sampling time T at t, $P(r_T)$ is the probability distribution of this quantity for random sample. Instantaneous emission rate could be expressed as the sum of a constant rate r_0 and a modulation whose frequency is $f(\tau)$ and depth is ε.

For a sine wave modulation of arbitrary frequency f, the instantaneous emission rate could be expressed as $r_0 +$

*Project supported by the National Basic Research Program of China (Grant Nos. 2012CB921603 and 2010CB923103), the National High Technology Research and Development Program of China (Grant No. 2011AA010801), the National Natural Science Foundation of China (Grant Nos. 11174187, 10934004, and 11204166), the International Science & Technology Cooperation Program of China (Grant No. 2001DFA12490), the NSFC Project for Excellent Research Team of China (Grant No. 61121064), the PCSIRT (Grant No. IRT 13076), and the Natural Science Foundation of Shanxi Province, China (Grant No. 2011091016).

†Corresponding author. E-mail: xlt@sxu.edu.cn

© 2014 Chinese Physical Society and IOP Publishing Ltd

$\varepsilon \sin(2\pi ft+\theta)$, so the effective photon emission rate is

$$r_T(t) = r_0 + \varepsilon\left(\frac{\sin \pi fT}{\pi fT}\right)\sin(2\pi ft + \pi fT + \theta). \quad (3)$$

During the sampling time T, the probability that n photons are detected is

$$\begin{aligned} p(n,T) &= \frac{(r_T T)^n}{n!}\mathrm{e}^{-r_T T} \\ &= \left\{\left[r_0+\varepsilon\left(\frac{\sin \pi fT}{\pi fT}\right)\sin(2\pi ft+\pi fT+\theta)\right]T\right\}^n \\ &\quad \times \mathrm{e}^{-\left\{\left[r_0+\varepsilon\left(\frac{\sin \pi fT}{\pi fT}\right)\sin(2\pi ft+\pi fT+\theta)\right]T\right\}}/n!. \end{aligned} \quad (4)$$

It is found that the probability for n photons to be detected $p(n)$ is related with the modulation frequency of the sine wave f. In other words, the SPM changes the probability for the photons to be detected.

Figure 1(a) illustrates that the photon distribution in weak laser with the photon emission rate being 0.1 obeys the Poisson distribution. It is shown that the probability of the two-photon occurrence is at the 10^{-3} level and the multiple-photon occurrence are almost zero, compared with the single-photon probability being about 0.1, so we take the weak light beam as single-photon stream. Figure 1(b) illustrates that the phase distribution of the photons detected follows the sine distribution when the incident photons are modulated by a sine wave within the sampling time T, which is n times of the sine wave duty t_0.

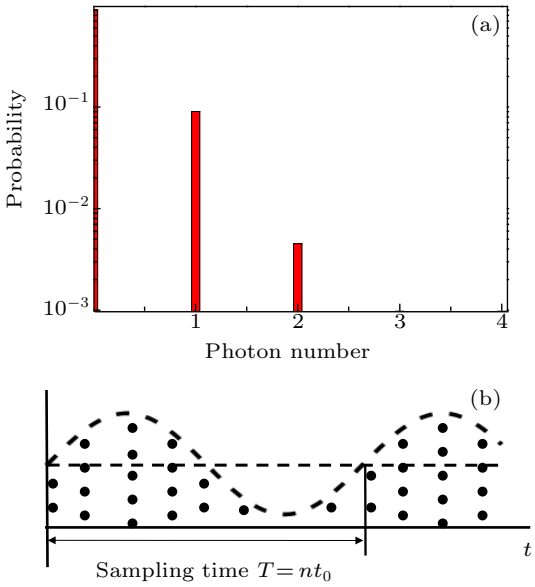


Fig. 1. (color online) SPM principle diagram. (a) The photon distribution in weak laser with the photon emission rate being $r_T = 0.1$ follow the Poisson distribution. (b) The phase distribution of the modulated photons obeys the sine distribution.

2.2. Square wave pulse FFT theory

According to the fast Fourier transform (FFT) theory, for a single square wave pulse, its FFT can be expressed as

$$x(f) = \int_{-\infty}^{\infty} x(t)\mathrm{e}^{-\mathrm{i}2\pi ft}\,\mathrm{d}t = A\tau\frac{\sin(\pi f\tau)}{\pi f\tau} = A\tau Sa(\pi f\tau), \quad (5)$$

where A is the amplitude of the pulse, and τ is the pulse width.

In consideration of the time shift characteristic of the FFT,

$$\begin{aligned} &x(f) = F[x(t)], \\ &F[x(t-t_0)] = x(f)\,\mathrm{e}^{-\mathrm{i}2\pi ft_0}, \\ &F[x(t+t_0)] = x(f)\,\mathrm{e}^{\mathrm{i}2\pi ft_0}. \end{aligned} \quad (6)$$

For instance, the FFT expression of the three square wave pulses with duty of T_d is

$$\begin{aligned} x(f) &= A\tau Sa(\pi f\tau)[1+\mathrm{e}^{\mathrm{i}2\pi fT_\mathrm{d}}+\mathrm{e}^{-\mathrm{i}2\pi fT_\mathrm{d}}] \\ &= A\tau Sa(\pi f\tau)[1+2\cos(2\pi fT_\mathrm{d})]. \end{aligned} \quad (7)$$

For $(2n+1)$ square wave pluses, its FFT expression is

$$\begin{aligned} x(f) &= A\tau Sa(\pi f\tau)\left[1+\mathrm{e}^{\mathrm{i}2\pi fT_\mathrm{d}}+\mathrm{e}^{-\mathrm{i}2\pi fT_\mathrm{d}}+\mathrm{e}^{\mathrm{i}2\pi f2T_\mathrm{d}}\right. \\ &\quad \left.+\mathrm{e}^{-\mathrm{i}2\pi f2T_\mathrm{d}}+\cdots+\mathrm{e}^{\mathrm{i}2\pi fnT_\mathrm{d}}+\mathrm{e}^{-\mathrm{i}2\pi fnT_\mathrm{d}}\right] \\ &= A\tau Sa(\pi f\tau)[1+2\cos(2\pi fnT_\mathrm{d})]. \end{aligned} \quad (8)$$

From Eq. (5), it is known that the spectrum of a single pulse is a periodic function. To calculate the frequency spectrum of a series of square wave pulses, it takes the frequency f as the horizontal axis, and the power $|x(f)|^2$ as the vertical axis. The spectra are discrete spectra that are also referred to as line spectra, and each line in the spectra represents each component of the series. Each line's peak ligature is called spectrum envelope, and reflects the harmonic component power as the frequency changing. The line interval is the reciprocal of pulse duty. The longer the pulse duty is, the smaller the line interval keeps and the denser the spectrum shows; on the contrary, the sparser the spectrum shows. Similar to the envelope, the interval envelope is the reciprocal of the pulse width. The wider the pulse width is, the smaller the envelope interval shows.

The square wave pulse is shown in Fig. 2(a), with the duty of T_d and the pulse width of τ. In Fig. 2(b), we show the FFT spectrum of the square wave pulse.

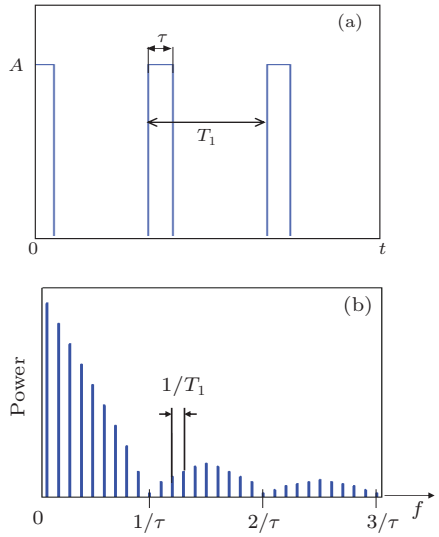


Fig. 2. (color online) (a) Square wave pulse and (b) its FFT spectrum.

3. Experimental setup

The experimental setup is illustrated in Fig. 3, where the laser beam is generated by a 1550-nm laser diode (1 kHz linewidth, NP photonics RELS), then emitted into the isolator, which is based on the Faraday rotation effect, to prevent the laser beams from being reflected back to the laser diode and damage the laser. Then, the laser enters into a continuous adjustable optical attenuator and to be attenuated to single photon level (the photon emission rate in the laser pulse is less than 0.1). The weak laser pulses are intensity modulated with an acoustic optical modulator (AOM, M200-2J-F2S Gooch & Housego) and then launched on an operating wavelength is 1550-nm gating single photon avalanche detector (SPAD, QCD300). The SPAD is external triggered by a pulse generator (SRS DG645) with 2-MHz repetition rate. The output pulse width is 500 ns and directly enters into the spectrum analysis (SA, Agilent E4402B) for the FFT spectrum analysis. The resolution band width of the SA is set as 1 kHz. The oscilloscope (OSC, LeCory 44MXs-B) is used to monitor the SPAD output. A function generator (Agilent 33250A) provides the sine-wave modulation signal for the AOM.

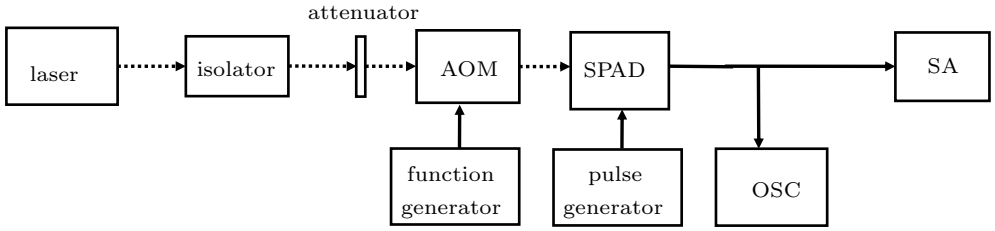


Fig. 3. Experimental setup diagram. AOM: acoustic optical modulator, SPAD: gating single photon avalanche detector, OSC: oscilloscope, SA: spectrum analysis.

4. Experimental results and analysis

4.1. Wide frequency spectrum analysis

Figure 4(a) illustrates the spectra on the SA when the sweep frequency range is 10 MHz. It can be found that there are some pits at the frequency of 2 MHz and the multiples of 2 MHz, i.e., there appears an envelope in each 2 MHz interval. In addition, as the mean photon number $\bar{n}$ increases, the power of the envelope increases.

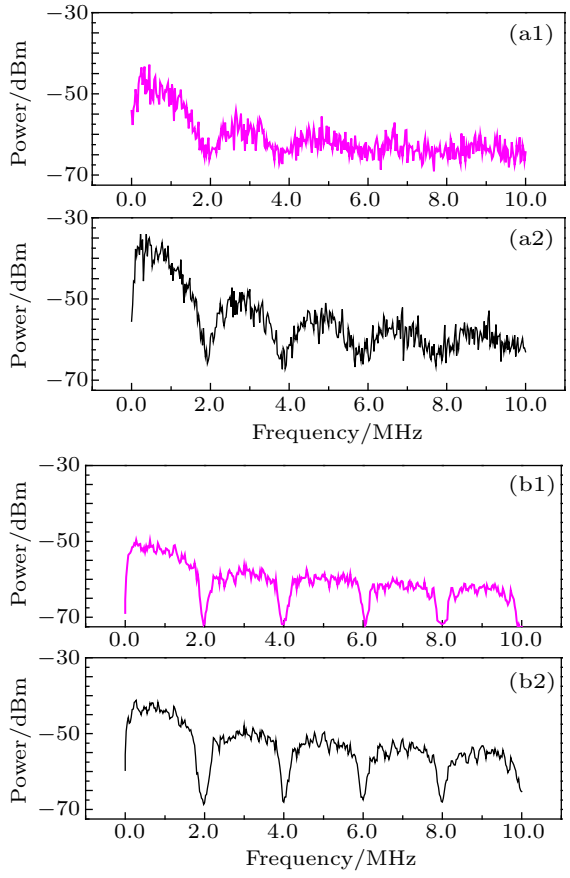


Fig. 4. (color online) The wide frequency spectrum experimental results with the mean photon number (a1) $\bar{n} = 2$ kcps and (a2) $\bar{n} = 14$ kcps; theoretical fitting results with the mean photon number (b1) $\bar{n} = 2$ kcps and (b2) $\bar{n} = 14$ kcps.

Figure 4(b) illustrates the theoretical fitting results. The theoretical fitting envelope interval is 2 MHz, which is the same as the experimental results. Since the mean photon number is the instantaneous value of the quantum fluctuations and the single photon appears randomly, the phenomenon that the mean photon number increases with the envelope amplitude is the same as the experimental results.

4.2. Signal analysis

We modulate the single photon by using the sine-wave modulation signal for the AOM with the repetition frequency $f_{\rm m} = 80$ kHz, the modulation depth is $\varepsilon \approx 1$ when peak-to-peak voltage $V_{\rm pp} = 300$ mV and offset voltage $V_{\rm offset} = 380$ mV. Figure 5(a) illustrates the spectra on the SA when the sweep frequency range is from 0 to 200 kHz. The initial peaks in Fig. 5(a) are from the $1/f$ noise measured by using the SA, that means the flicker noise. There is an obvious peak at the frequency of the modulation sine wave of 80 kHz, and the peak power increases as the mean photon number increases. We present the spectrum for $\bar{n} = 4$ kcps, and the signal power is -43.7 dBm, with the resolution band width of the SA being 1 kHz, the background noise power being -72.53 dBm/$\sqrt{\rm Hz}$ (Fig. 5(a1)); the spectrum for $\bar{n} = 40$ kcps, with the signal power being -28.8 dBm, the noise power being -63.73 dBm/$\sqrt{\rm Hz}$ (Fig. 5(a2)); and the spectrum for $\bar{n} = 80$kcps, with the signal power being -21.6 dBm, the noise power being -59.64 dBm/$\sqrt{\rm Hz}$ (Fig. 5(a3)).

Figure 5(b) illustrates the corresponding theoretical fitting results. We present the spectrum for $\bar{n} = 4$ kcps, with the signal power being -40.7 dBm, the noise power being -73.6 dBm/$\sqrt{\text{Hz}}$ (Fig. 5(b1)); the spectrum for $\bar{n} = 40$ kcps, with the signal power being -27.99 dBm, the noise power being -63.35 dBm/$\sqrt{\text{Hz}}$ (Fig. 5(b2)); and the spectrum for $\bar{n} = 80$ kcps, with the signal power being -22.5 dBm, the noise power being -60.85 dBm/$\sqrt{\text{Hz}}$ (Fig. 5(b3)). It is obvious that the signal power increases with the mean photon number both theoretically and experimentally.

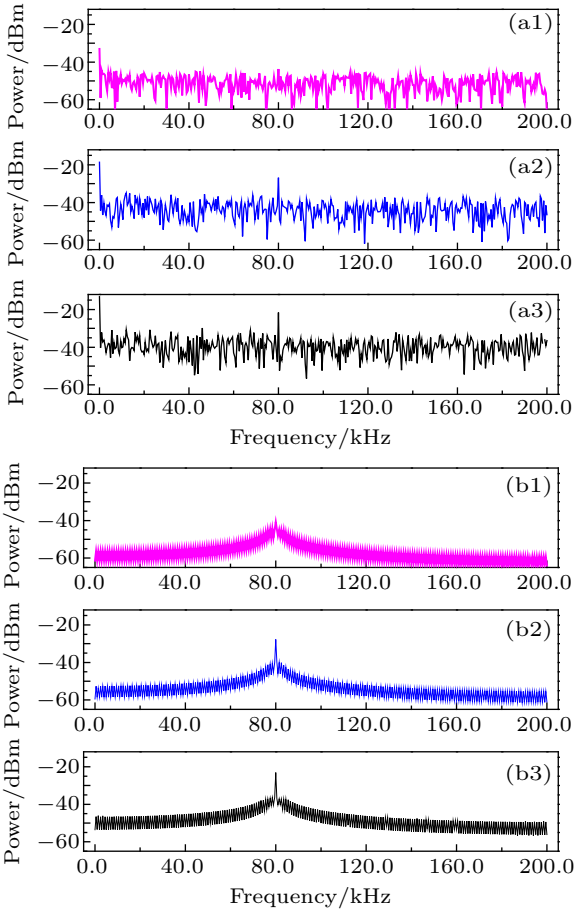


Fig. 5. (color online) The experimental results of signal spectrum for the mean photon number (a1) $\bar{n} = 4$ kcps, (a2) $\bar{n} = 40$ kcps, and (a3) $\bar{n} = 80$ kcps; the theoretical fitting results of signal spectrum for the mean photon number (b1) $\bar{n} = 4$ kcps, (b2) $\bar{n} = 40$ kcps, and (b3) $\bar{n} = 80$ kcps. The modulation frequency is 80 kHz.

4.3. SNR analysis and the power-frequency characteristic of the SPM

In the experiment, the noises are mainly divided into the following kinds on the base of the devices in the system: flicker noise, thermal noise and shot noise, and the shot noise occupies the main composition.[17] Shot noise mainly originates from the fluctuation of the experimental outcomes because there exist few electrons or photons statistical fluctuations in the photoelectric detector. It is affected by the quantum fluctuations at high frequencies. Normally, we take it as the form of white noise with the same power density at arbitrary frequencies. The shot noise in the system mainly contains the following four categories: (i) P–N junction shot noise, it is emerged due to the stochastic diffraction of carriers in the semiconductor; (ii) signal light photon noise, it is produced because of the photons random excitation carriers in the light filed and the carriers stochastic fluctuation; (iii) background light photon noise, it is caused by the background light produce little photons leads to the deviation; (iv) dark current shot noise, it exists owing to the dark current in single photon detector that leads to the output signal fluctuations. Here, the contributing background noises are mainly the signal light photon noise and the dark current shot noise. As both of them obeys the Poisson distribution,[15] there will show the white noise characteristics in the spectrum.

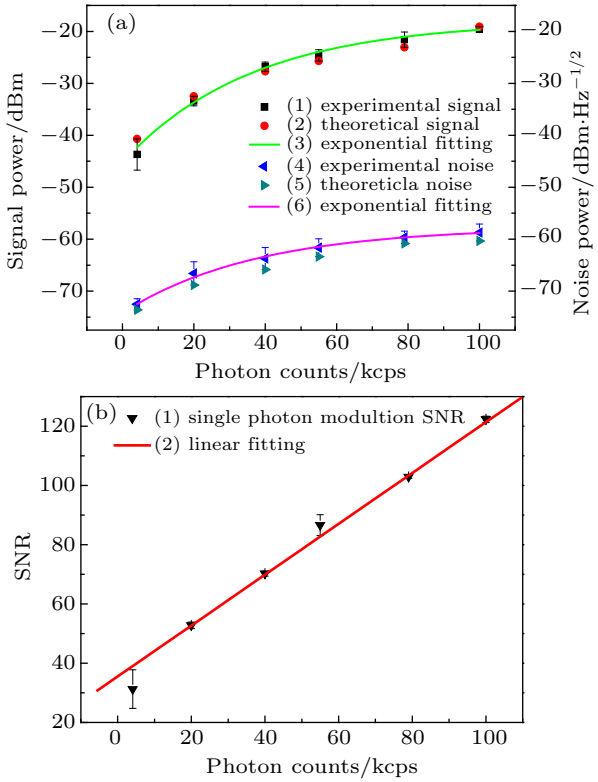


Fig. 6. (color online) The experimental result analysis. (a) The experimentally and theoretically determined values of modulation signal power and noise power as a function of the mean photon number. The solid lines show the theoretical fitting as given by Eq. (9). The error bar is from the noise power variation. (b) The linear relationship between the SNR and the mean photon number.

Analyzing the signal power and the background noise in the theoretical fitting and the experimental, the results are shown in Fig. 6(a). We find that the theoretical fitting results coincide well with the experimental results. In Fig. 6(a), the exponential fitting curve (3) shows the fitting results of the modulation signal as a function of the incident photons. Similar to the magenta curve (6), it is the fitting results of the background noise in the experiment as a function of the incident photons. The error bar comes from the power variation. The fitting equation of the two curves is

$$y = a\exp(-x/x_0) + y_0, \tag{9}$$

where the fitting determination coefficient squares are all up to 0.99, indicating good fitting results. The coefficient x_0 in the curves (3) and (6) is 36.261 kcps and 37.412 kcps, respectively.

We calculate the SNR in the experiment and it is shown in Fig. 6(b). The SNR is up to 122 and the slop of the line (2) is 0.8649 per photon. The error bars are from the background variation.

From the above analysis, we can see that although the noise is increasing with the mean photon number and the same as the signal in the experiment, the SNR is linear increasing as the mean photon number increased.

Changing the modulation frequency, we obtain the power-frequency characteristics of the modulation signal on the SA, as shown in Fig. 7. It is found that the modulation frequency is up to 1800 kHz, considering the background noise power of -60.85 dBm/$\sqrt{\text{Hz}}$ when $\bar{n} = 80$ kcps. It turns out that the SPM method has high adaptive capacity for the high-frequency modulation.

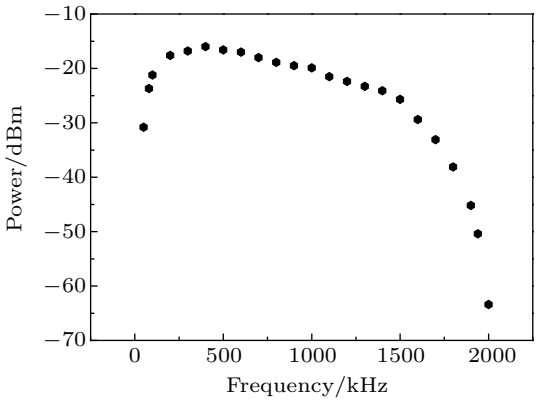


Fig. 7. The power-frequency characteristic for the SPM when the mean photon number $\bar{n} = 80$ kcps.

5. Summary

This paper introduces the measurement of the modulation signal spectrum by using the SPM method. It is found that the SNR shows linear growth in the analysis of the measured SNR. Moreover, we take the theoretical calculations of the spectrum, and it is shown that the calculation results coincide well with the experimental results. It is shown that the SPM method can indeed substantially realize both in measuring the modulation signal at high frequencies and obtaining high SNR.

The benefits of the SPM method are that it not only could be exploited potentially for sensitive detection, but also enables fast real-time tracking at single photon level. By using of lock-in amplifier, the SPM has potential applications in enhancing the detection efficiency with the optimizing threshold for single photon detection,[18] and in realizing the fast locking of the Fabry–Perot cavity to a single-photon frequency.[19]

References

[1] Hadfield R H 2009 *Nat. Photon.* **3** 696
[2] Liu Y, Wu Q L, Han Z F, Dai Y M and Guo G C 2010 *Chin. Phys. B* **19** 080308
[3] Gu M and Sheppard C J R 1995 *J. Microsc.* **177** 128
[4] Lee C G, Moon I and Javidi B 2012 *J. Opt. Soc. Am. A* **29** 854
[5] Lacaita A L, Francese P A and Cova S D 1993 *Opt. Lett.* **18** 1110
[6] Wang X B, Wang J J, Zhang G F, Xiao L T and Jia S T 2011 *Chin. Phys. B* **20** 064204
[7] Zhou X Y, Wang L J and Mandel L 1991 *Phys. Rev. Lett.* **67** 318
[8] Kwiat P G, Stcinbcrg A M and Chiao R Y 1993 *Phys. Rev. A* **48** R867
[9] Takeuchi S, Kim J, Yamamoto Y and Hogue H H 1999 *Appl. Phys. Lett.* **74** 1063
[10] Arecchi F T, Gatti E and Sona A 1966 *Rev. Sci. Instrum.* **37** 942
[11] Alfano R R and Ockmanc N 1968 *J. Opt. Soc. Am. A* **58** 90
[12] Pelissier B and Sadeghi N 1996 *Rev. Sci. Instrum.* **67** 3405
[13] Braun B and Libchaber A 2002 *Opt. Lett.* **27** 1418
[14] Pulford D, Robillard C and Huntington E 2005 *Rev. Sci. Instrum.* **76** 063114
[15] Huang T, Dong S L, Guo X J, Xiao L T and Jia S T 2006 *Appl. Phys. Lett.* **89** 061102
[16] Mandel L 1958 *Proc. Phys. Soc.* **72** 1037
[17] Raouf S S, Sadik A R, Wafi N K and Aboud K M 1986 *Astrophys. Space Sci.* **127** 207
[18] Wang X B, Zhang G F, Chen R Y, Gao Y, Xiao L T and Jia S T 2012 *Opt. Laser Technol.* **44** 1773
[19] Wang J J, He B, Yu B, Liu Y, Wang X B, Xiao L T and Jia S T 2012 *Acta Phys. Sin.* **61** 204203 (in Chinese)